Nuclear deformation and shape coexistence

Kasia Hadyńska-Klęk

INFN Laboratori Nazionali di Legnaro

3rd COULEX School, INFN LNL, 28-30.11.2016

Nuclear shapes - examples

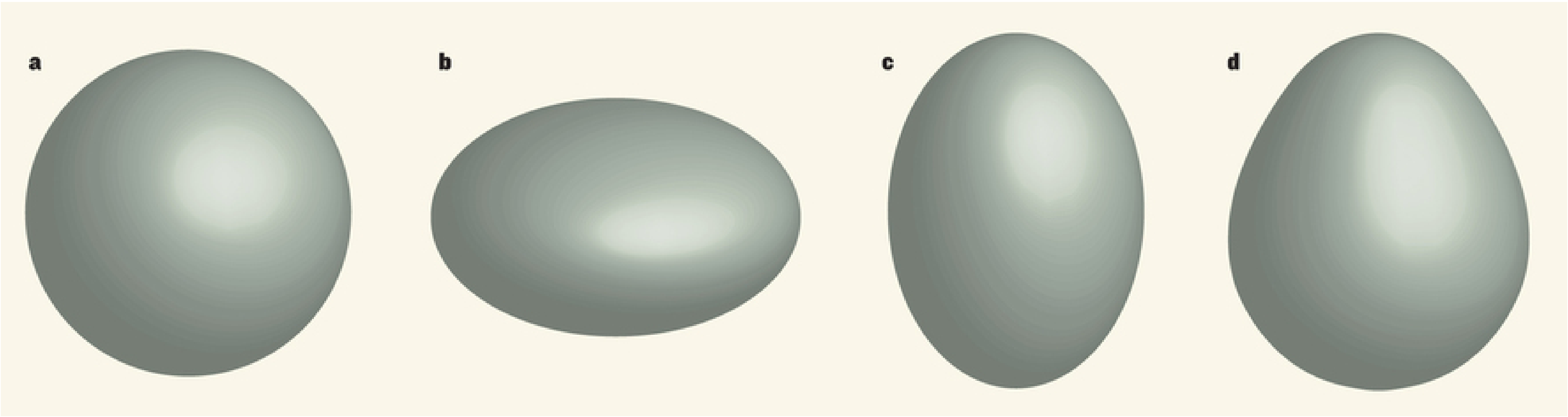

sphere oblate prolate octupole deformed

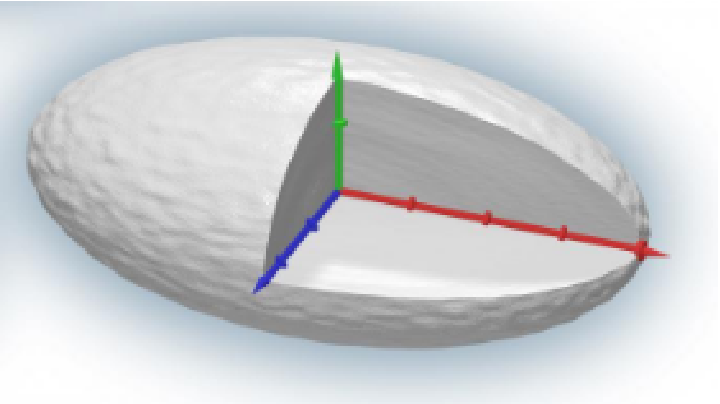

prolate triaxial

More!

Coulomb excitation is a precise tool to measure collectivity of nuclear excitations – in particular **nuclear shapes**

The observables related to the quadrupole collectivity and shape of a nucleus are:

- the reduced transition probabilities

- spectroscopic quadrupole moments

Shape coexistance

Presence at low energy near-degenerate states in atomic nucleus characterized by different shape.

Interplay between two opposing tendencies

- Stabilizing effect of closed shells (subshells) → sphericity
- Residual proton-neutron interaction → deformation

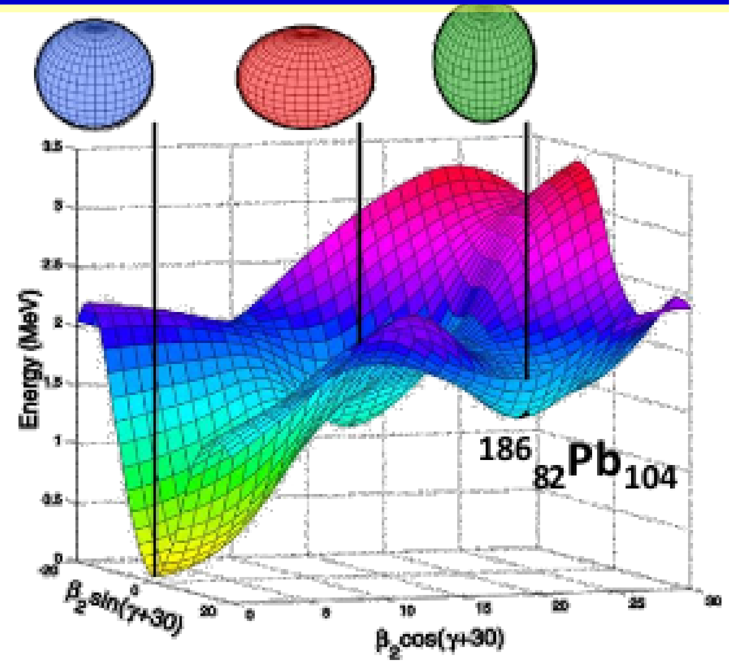

A. Andreyev et al Nature 405:430 (2000)

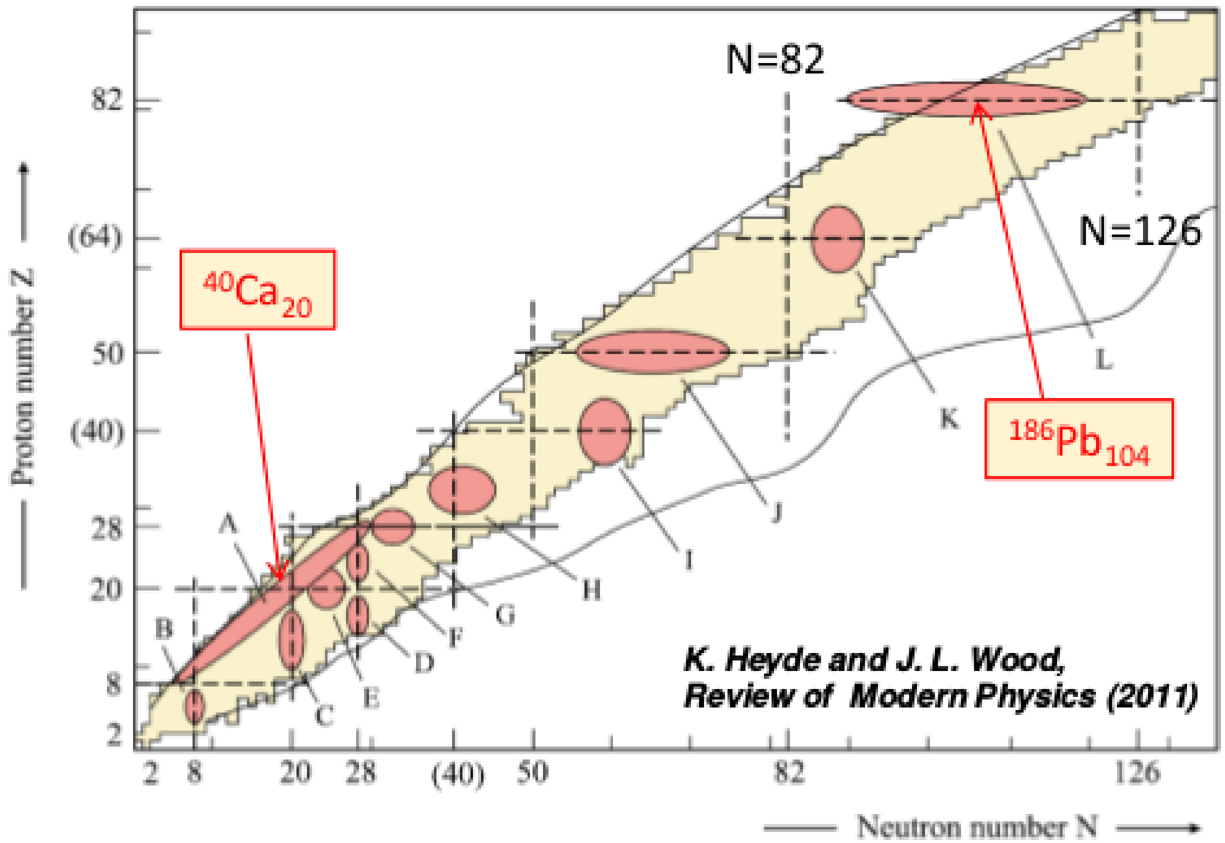

K. Heyde and J. L. Wood, Review of Modern Physics (2011)

Shape coexistence at and around closed proton and/or neutron (sub)shells.

What do we measure?

1. The level scheme
→ low-lying 0^+ states.

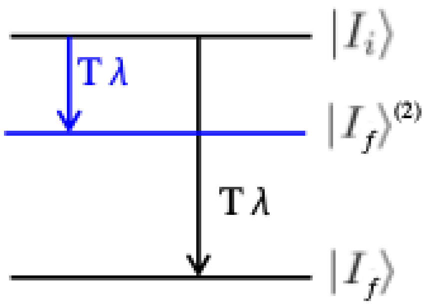

2. E0 transitions, $\rho^2(E0)$:

$\rho^2(E0) = (Z^2/R_0^4) \cdot \alpha^2 \cdot \beta^2\, [\Delta\langle r^2\rangle]^2$

→ wave function mixing,

3. Reduced transition probabilities , B(E2).

$$P(T\lambda; I_i \to I_f) = \frac{8\pi(\lambda+1)}{\lambda\,((2\lambda+1)!!)^2}\frac{1}{\hbar}\left(\frac{E_\gamma}{\hbar c}\right)^{2\lambda+1} \cdot B(T\lambda; I_i \to I_f)$$

$$B(T\lambda; I_i \to I_f) = \frac{1}{2I_i+1}|\langle I_f||\hat{M}(T\lambda)||I_i\rangle|^2$$

4. Quadrupole moments Q.

What do we measure?

1. The level scheme

→ low-lying 0^+ states.

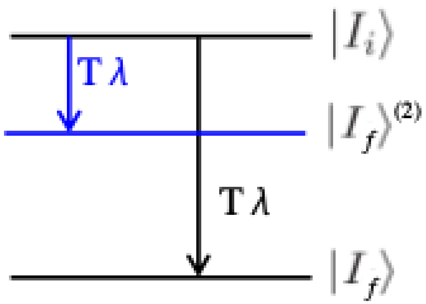

2. E0 transitions, $\rho^2(E0)$:

$\rho^2(E0) = (Z^2/R_0^4) \cdot \alpha^2 \cdot \beta^2 \, [\Delta\langle r^2\rangle]^2$

→ wave function mixing,

3. Reduced transition probabilities , B(E2).

$$P(T\lambda; I_i \to I_f) = \frac{8\pi(\lambda+1)}{\lambda\left((2\lambda+1)!!\right)^2}\frac{1}{\hbar}\left(\frac{E_\gamma}{\hbar c}\right)^{2\lambda+1} \cdot B(T\lambda; I_i \to I_f)$$

$$B(T\lambda; I_i \to I_f) = \frac{1}{2I_i+1}|\langle I_f\|\hat{M}(T\lambda)\|I_i\rangle|^2$$

4. Quadrupole moments Q.

DEFORMATION

Coulomb excitation and nuclear shapes

Quadrupole Sum Rules

- Electric multipole transition operator, **E(λ,μ)**, is a **spherical tensor** and its zero-coupled products can be formed, which are **rotationally invariant** – they are identical and describe nuclear shape in both intrinsic frame and the laboratory frame

- The following parametrization of E2 operator is general, model independent and analogous to expressing the radial shape of a **quadrupole-deformed object** in terms of Bohr's shape parameters (β,γ)

$$E(2,0) = Qcos\delta$$

$$E(2,1) = E(2,-1) = 0$$

$$E(2,2) = E(2,-2) = (1/\sqrt{2}) \cdot Qsin\delta$$

- Using this parametrization the **zero-coupled products of the E2 operators** can be formed in terms of **Q and δ**

$$[E2 \times E2]^0 = \frac{1}{\sqrt{5}} Q^2$$

$$\left\{ [E2 \times E2]^2 \times E2 \right\}^0 = \frac{\sqrt{2}}{\sqrt{35}} Q^3 \cos 3\delta$$

- the matrix elements of the E2 operator products can be evaluated using the **basic intermediate state expansion**

$$\left\langle s \left| (E2 \times E2)^J \right| r \right\rangle = \frac{(-1)^{I_s+I_r}}{(2I_s+1)^{1/2}} \sum_t \langle s||E2||t\rangle \langle t||E2||r\rangle \left\{ \begin{array}{ccc} 2 & 2 & J \\ I_s & I_r & I_t \end{array} \right\}$$

Quadrupole Sum Rules – nuclear shapes

- Now let's combine the approaches:

$$\frac{\langle Q^2 \rangle}{\sqrt{5}} = \left\langle \mathrm{i} \,\|[E2 \times E2]_0\|\, \mathrm{i} \right\rangle$$
$$= \frac{(-1)^{2I_i}}{\sqrt{(2I_i+1)}} \cdot \sum_t \left\langle \mathrm{i} \| E2 \| t \right\rangle \left\langle t \| E2 \| \mathrm{i} \right\rangle \begin{Bmatrix} 2 & 2 & 0 \\ I_i & I_i & I_t \end{Bmatrix},$$

and

$$\sqrt{\frac{2}{35}} \langle Q^3 \cos(3\delta) \rangle = \left\langle \mathrm{i} \,\left\| \left[[E2 \times E2]_2 \times E2 \right]_0 \right\|\, \mathrm{i} \right\rangle$$
$$= \frac{(\pm 1)}{(2I_i+1)} \cdot \sum_{t,u} \left\langle \mathrm{i} \| E2 \| u \right\rangle \left\langle u \| E2 \| t \right\rangle \left\langle t \| E2 \| \mathrm{i} \right\rangle \begin{Bmatrix} 2 & 2 & 2 \\ I_i & I_t & I_u \end{Bmatrix},$$

In practice..

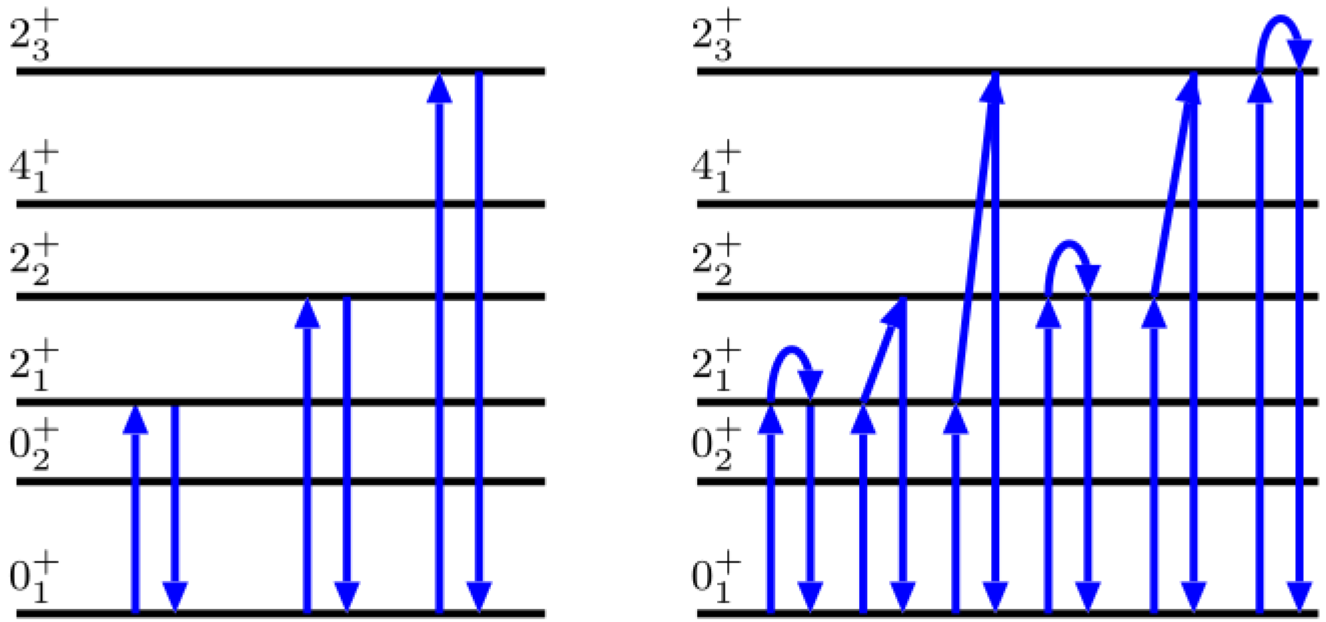

Figure 7. A schematic illustration of an example products of $E2$ matrix elements taken into account to calculate lowest order invariants: $\langle Q^2 \rangle$ (left) and $\langle Q^3 \cos(3\delta) \rangle$ (right) for the case of the 0^+ ground state of even–even nucleus.

In practice..

K. WRZOSEK-LIPSKA *et al.* PHYSICAL REVIEW C **86**, 064305 (2012)

TABLE IX. Contribution of individual matrix elements to the values of the $\langle 0_1^+|Q^2|0_1^+\rangle$ and $\langle 0_2^+|Q^2|0_2^+\rangle$ invariants in ^{100}Mo. The $\sqrt{5}\times\left\{\begin{smallmatrix}2 & 2 & 0\\ 0 & 0 & 2\end{smallmatrix}\right\}$ factor, multiplying the contributions according to Eqs. (3) and (4), is in this case equal to 1.

State	Component $E2\times E2$	Contribution to $\langle Q^2\rangle$ (e^2b^2)
	$\langle 0_1^+\|E2\|2_1^+\rangle\langle 2_1^+\|E2\|0_1^+\rangle$	0.46
0_1^+	$\langle 0_1^+\|E2\|2_2^+\rangle\langle 2_2^+\|E2\|0_1^+\rangle$	0.01
	$\langle 0_1^+\|E2\|2_3^+\rangle\langle 2_3^+\|E2\|0_1^+\rangle$	0.0002
	$\langle 0_1^+\|Q^2\|0_1^+\rangle$	0.47(3)
	$\langle 0_2^+\|E2\|2_1^+\rangle\langle 2_1^+\|E2\|0_2^+\rangle$	0.26
0_2^+	$\langle 0_2^+\|E2\|2_2^+\rangle\langle 2_2^+\|E2\|0_2^+\rangle$	0.10
	$\langle 0_2^+\|E2\|2_3^+\rangle\langle 2_3^+\|E2\|0_2^+\rangle$	0.25
	$\langle 0_2^+\|Q^2\|0_2^+\rangle$	0.62(3)

In practice..

K. WRZOSEK-LIPSKA *et al.* PHYSICAL REVIEW C **86**, 064305 (2012)

TABLE X. Contribution of individual matrix elements to the values of the $\langle 0_1^+|Q^3\cos(3\delta)|0_1^+\rangle$ and $\langle 0_2^+|Q^3\cos(3\delta)|0_2^+\rangle$ invariants in ^{100}Mo. Presented invariants, accordingly to Eqs. (5) and (6), result from the multiplication of the sum of all contributions by the factor $(-1)\times\sqrt{\frac{35}{2}}\times\left\{\begin{smallmatrix}2&2&2\\0&2&2\end{smallmatrix}\right\}$, equal to -0.837.

State	Component $E2\times E2\times E2$	Contribution to $\langle Q^3\cos 3\delta\rangle$ (e^3b^3)
	$\langle 0_1^+\|E2\|2_1^+\rangle\langle 2_1^+\|E2\|2_1^+\rangle\langle 2_1^+\|E2\|0_1^+\rangle$	−0.155
	$\langle 0_1^+\|E2\|2_1^+\rangle\langle 2_1^+\|E2\|2_2^+\rangle\langle 2_2^+\|E2\|0_1^+\rangle$	0.132
	$\langle 0_1^+\|E2\|2_1^+\rangle\langle 2_1^+\|E2\|2_3^+\rangle\langle 2_3^+\|E2\|0_1^+\rangle$	0.002
0_1^+	$\langle 0_1^+\|E2\|2_2^+\rangle\langle 2_2^+\|E2\|2_2^+\rangle\langle 2_2^+\|E2\|0_1^+\rangle$	0.013
	$\langle 0_1^+\|E2\|2_2^+\rangle\langle 2_2^+\|E2\|2_3^+\rangle\langle 2_3^+\|E2\|0_1^+\rangle$	−0.001
	$\langle 0_1^+\|E2\|2_3^+\rangle\langle 2_3^+\|E2\|2_3^+\rangle\langle 2_3^+\|E2\|0_1^+\rangle$	−0.0001
	Sum of all contributions	−0.009
	$\langle 0_1^+\|Q^3\cos(3\delta)\|0_1^+\rangle$	0.01(6)
	$\langle 0_2^+\|E2\|2_1^+\rangle\langle 2_1^+\|E2\|2_1^+\rangle\langle 0_2^+\|E2\|2_1^+\rangle$	−0.09
	$\langle 0_2^+\|E2\|2_1^+\rangle\langle 2_1^+\|E2\|2_2^+\rangle\langle 2_2^+\|E2\|0_2^+\rangle$	−0.31
	$\langle 0_2^+\|E2\|2_1^+\rangle\langle 2_1^+\|E2\|2_3^+\rangle\langle 2_3^+\|E2\|0_2^+\rangle$	−0.04
0_2^+	$\langle 0_2^+\|E2\|2_2^+\rangle\langle 2_2^+\|E2\|2_2^+\rangle\langle 2_2^+\|E2\|0_2^+\rangle$	0.12
	$\langle 0_2^+\|E2\|2_2^+\rangle\langle 2_2^+\|E2\|2_3^+\rangle\langle 2_3^+\|E2\|0_2^+\rangle$	−0.13
	$\langle 0_2^+\|E2\|2_3^+\rangle\langle 2_3^+\|E2\|2_3^+\rangle\langle 2_3^+\|E2\|0_2^+\rangle$	−0.06
	Sum of all contributions	−0.51
	$\langle 0_2^+\|Q^3\cos(3\delta)\|0_2^+\rangle$	0.42(6)

Quadrupole Sum Rules – nuclear shapes

- The lowest-order products of **E2** operator provide information on the **intrinsic quadrupole deformation parameters** of a nucleus:

  - the **overall quadrupole deformation (Q^2)**

  - the **non-axiality parameter (cos(3δ))**:

    cos(3δ)=-1 OBLATE,
    cos(3δ)=1 PROLATE,
    cos(3δ)=0 TRIAXIAL

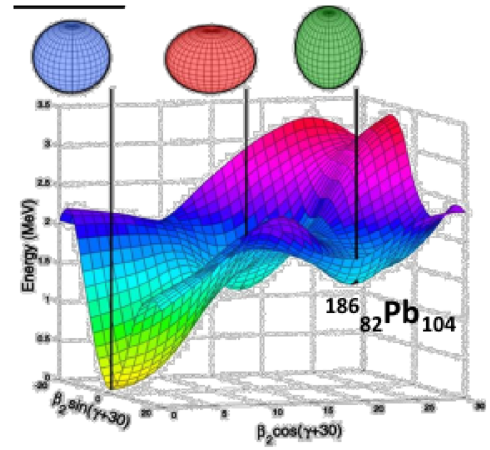

A. Andreyev et al Nature 405:430 (2000)

- Higher order rotational invariants can be formed with the different *J* couplings, involving summation over different sets of the reduced E2 matrix elements

Prolate, oblate, spherical? Or triaxial?

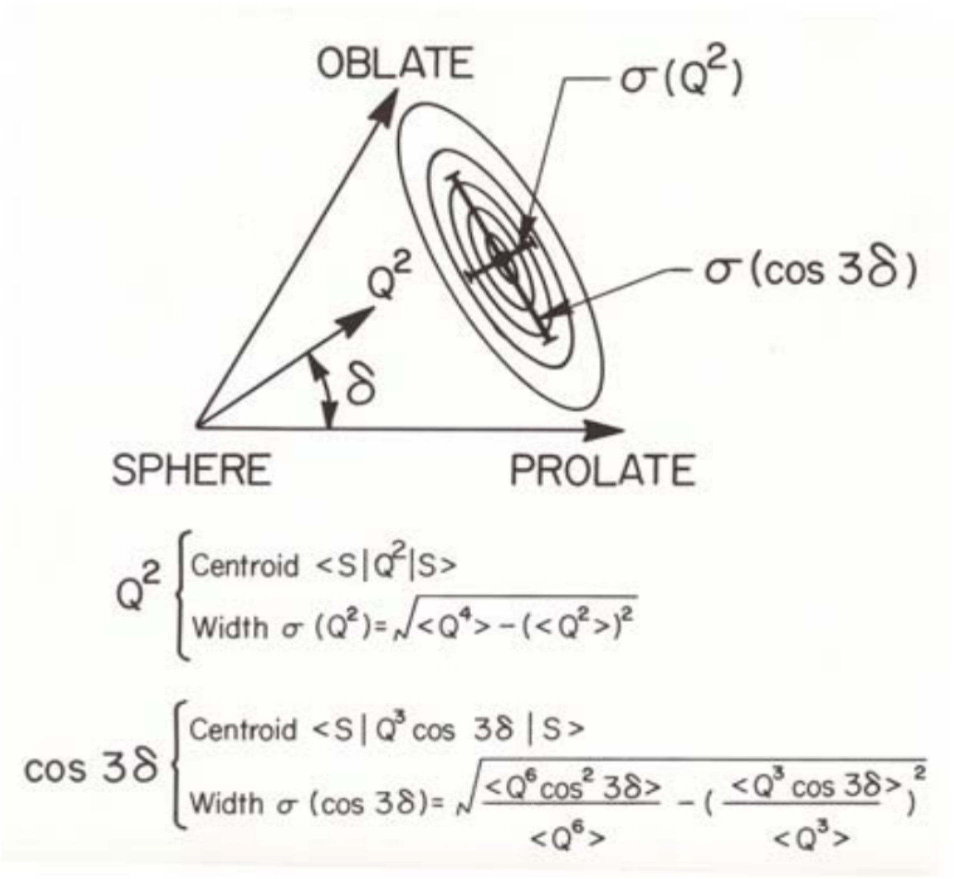

1. The sum rules derived from the rotational invariants allow measurement of the **expectation values** of rotational invariants built of **Q and δ**

2. It is possible to find the s**tatistical distribution of Q^2 and cos3δ** i.e. the first statistical moments related to the **softness** in both parameters

SHAPE PARAMETERS

$$\frac{1}{\sqrt{5}}\langle Q^2\rangle = \frac{1}{\sqrt{2I_i+1}}\sum_t \langle i\|E2\|t\rangle\langle t\|E2\|f\rangle \begin{Bmatrix}2 & 2 & 0\\ I_i & I_f & I_t\end{Bmatrix}$$

$$\langle Q^3\cos(3\delta)\rangle = \mp\frac{\sqrt{35}}{\sqrt{2}}\frac{1}{\sqrt{2I_i+1}}\sum_{tu}\langle s\|E2\|u\rangle\langle u\|E2\|t\rangle\langle t\|E2\|s\rangle \begin{Bmatrix}2 & 2 & 2\\ I_s & I_t & I_u\end{Bmatrix}$$

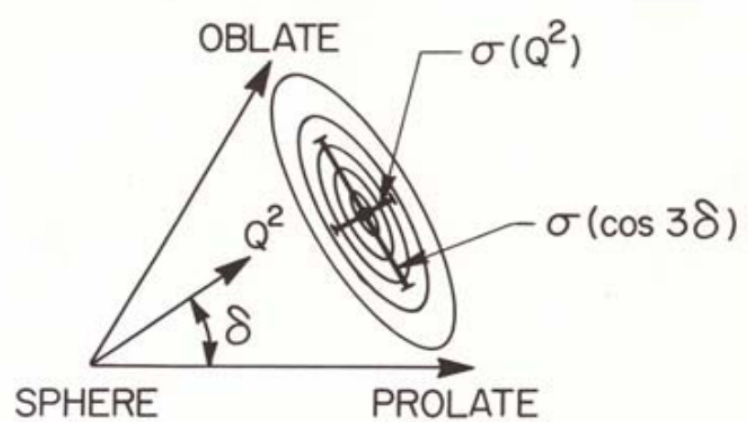

Q^2 { Centroid $<S|Q^2|S>$; Width $\sigma(Q^2) = \sqrt{<Q^4> - (<Q^2>)^2}$ }

$\cos 3\delta$ { Centroid $<S|Q^3\cos 3\delta|S>$; Width $\sigma(\cos 3\delta) = \sqrt{\frac{<Q^6\cos^2 3\delta>}{<Q^6>} - \left(\frac{<Q^3\cos 3\delta>}{<Q^3>}\right)^2}$ }

$$\beta = \sqrt{\langle\beta^2\rangle} = \sqrt{\frac{\langle Q^2\rangle}{q_0^2}},$$

$$\gamma = \arccos\langle\cos(3\delta)\rangle,$$

J. Srebrny and D. Cline, Int. J. Mod. Phys. E20, 422 (2011)

Shape coexistence in ^{42}Ca

Nuclear shapes in ^{42}Ca

Superdeformed band in ^{40}Ca (DSAM, ANL)

$B(E2; 4^+ \rightarrow 2^+) = 170$ Wu
Q_t=1.80(+10.39,-0.29) eb
β_2=0.59(+0.11,-0.07)

E. Ideguchi et al., PRL 87, 222501 (2001),
C.J. Chiara et al., PRC 67, 041303R (2003)

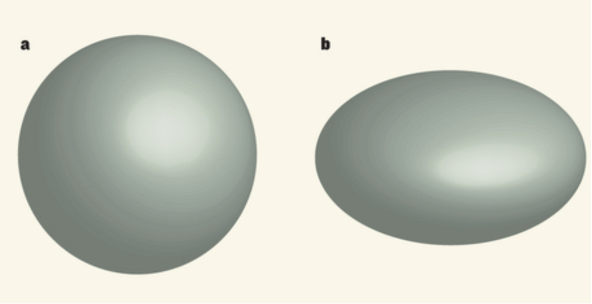

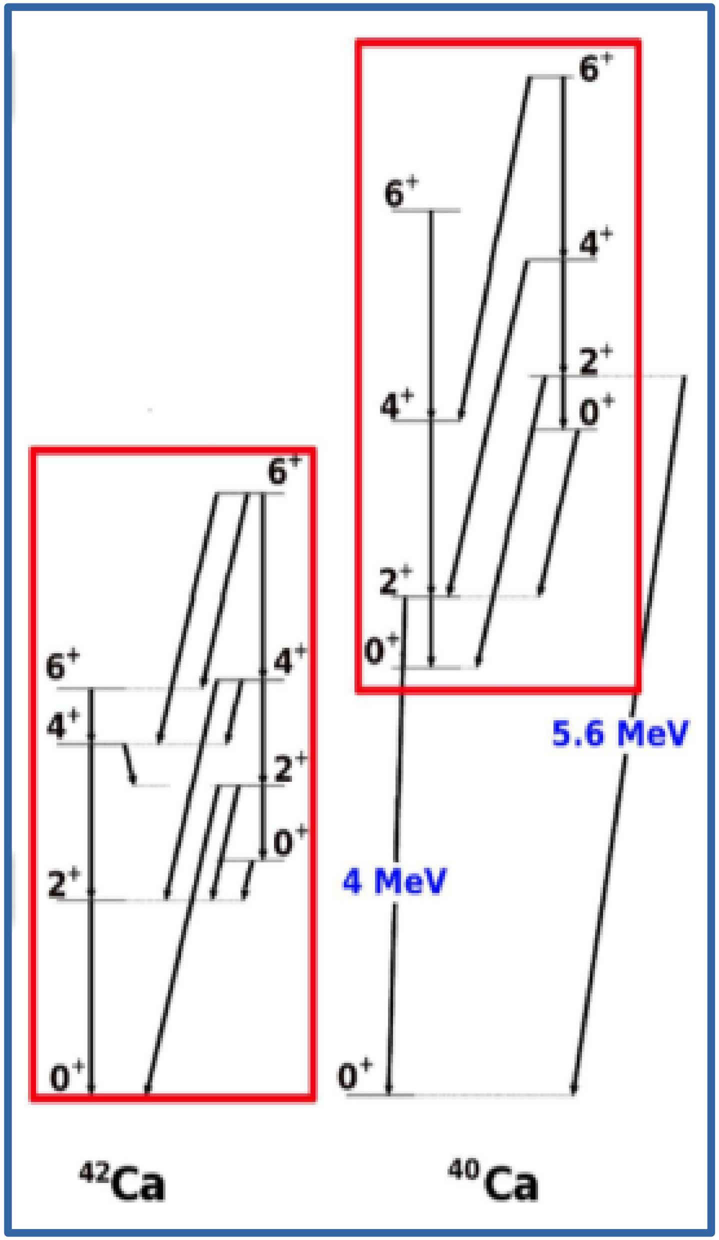

COULEX of ^{42}Ca

- INFN LNL
- Beam: ^{42}Ca, 170 MeV
- Targets:
  - ^{208}Pb, 1 mg/cm^2
  - ^{197}Au, 1 mg/cm^2
- AGATA: 3 triple clusters, 143.8 mm from the target
- DANTE: 3 MCP detectors, 100-144^o

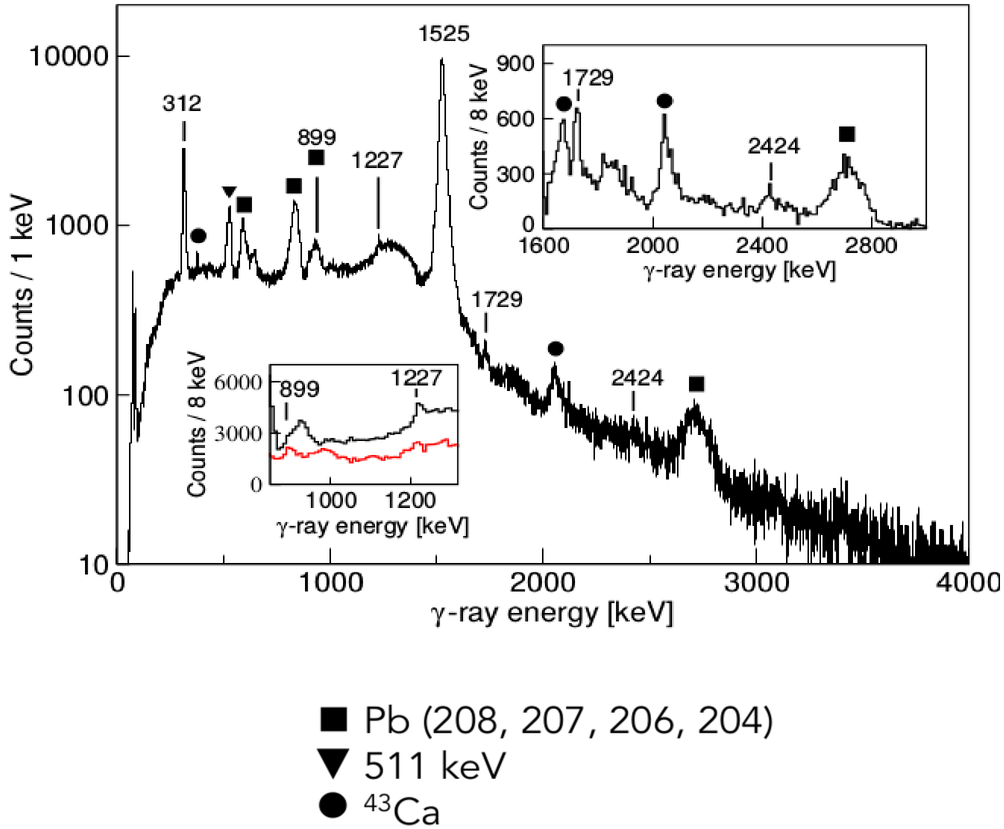

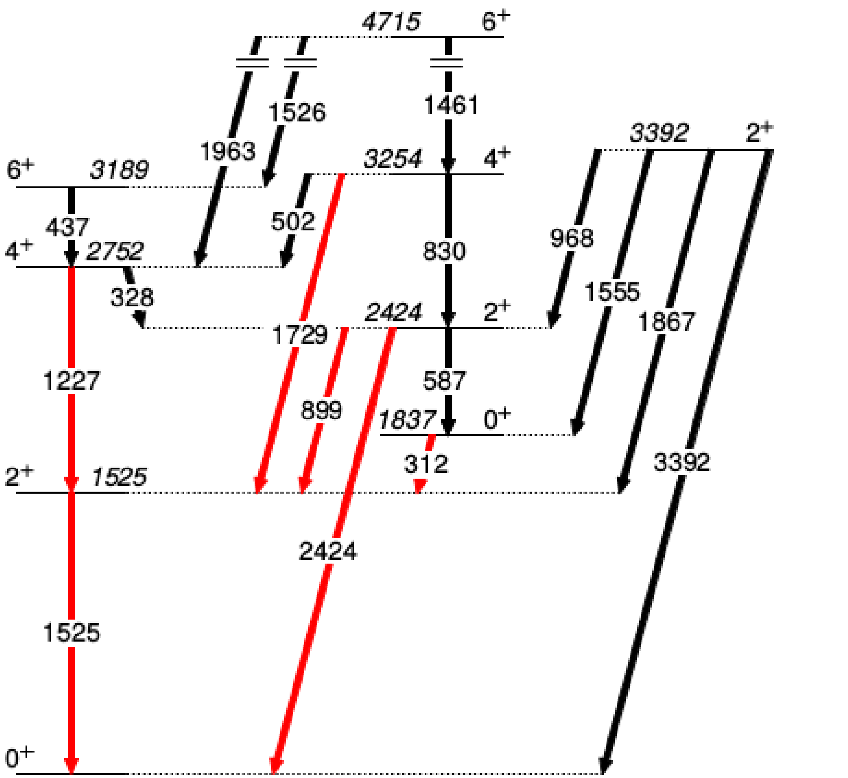

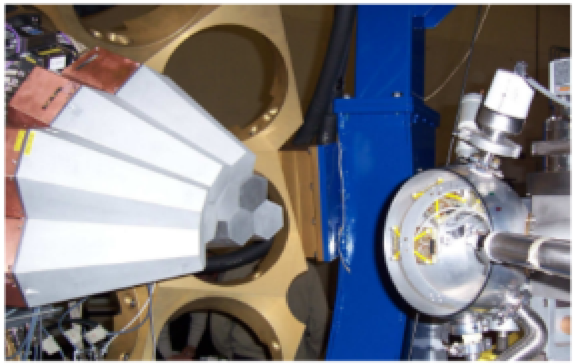

GOSIA analysis - ^{42}Ca

$I_i^+ \to I_f^+$	$\langle I_i \| E2 \| I_f \rangle$ [e fm^2] Present	$B(E2\downarrow; I_i^+ \to I_f^+)$ [W.u.] Present	$B(E2\downarrow; I_i^+ \to I_f^+)$ [W.u.] Previous
$2_1^+ \to 0_1^+$	$20.5^{+0.6}_{-0.6}$	$9.7^{+0.6}_{-0.6}$	9.3 ± 1 [36] 11 ± 2 [28] 9 ± 3 [27] 8.5 ± 1.9 [45]
$4_1^+ \to 2_1^+$	$24.3^{+1.2}_{-1.2}$	$7.6^{+0.7}_{-0.7}$	50 ± 15 [28] 11 ± 3 [27] 10^{+10}_{-8} [45]
$6_1^+ \to 4_1^+$	$9.3^{+0.2}_{-0.2}$	$0.77^{+0.03}_{-0.03}$	0.7 ± 0.3 [27]
$0_2^+ \to 2_1^+$	$22.2^{+1.1}_{-1.1}$	57^{+6}_{-6}	64 ± 4 [27] 100 ± 6 [28] 55 ± 1 [42] 64 ± 4 [45]
$2_2^+ \to 0_1^+$	$-6.4^{+0.3}_{-0.3}$	$1.0^{+0.1}_{-0.1}$	2.2 ± 0.6 [28] 1.5 ± 0.5 [27] 1.2 ± 0.3 [45]
$2_2^+ \to 2_1^+$	$-23.7^{+2.3}_{-2.7}$	$12.9^{+2.5}_{-2.5}$	17 ± 11 [28] 19^{+22}_{-14} [27] 14^{+35}_{-9} [45]
$4_2^+ \to 2_1^+$	42^{+3}_{-4}	23^{+3}_{-4}	30 ± 11 [28] 16 ± 5 [27] 12^{+7}_{-4} [45]
$2_2^+ \to 0_2^+$	26^{+5}_{-3}	15^{+6}_{-4}	< 61 [27] < 46 [45]
$4_2^+ \to 2_2^+$	46^{+3}_{-6}	27^{+4}_{-6}	60 ± 30 [27] 60 ± 20 [28] 40^{+40}_{-30} [45]
	$\langle I_i \| E2 \| I_f \rangle$ [e fm^2]	Q_{sp} [e fm^2]	
$2_1^+ \to 2_1^+$	-16^{+9}_{-3}	-12^{+7}_{-2}	-19 ± 8 [36]
$2_2^+ \to 2_2^+$	-55^{+15}_{-15}	-42^{+12}_{-12}	

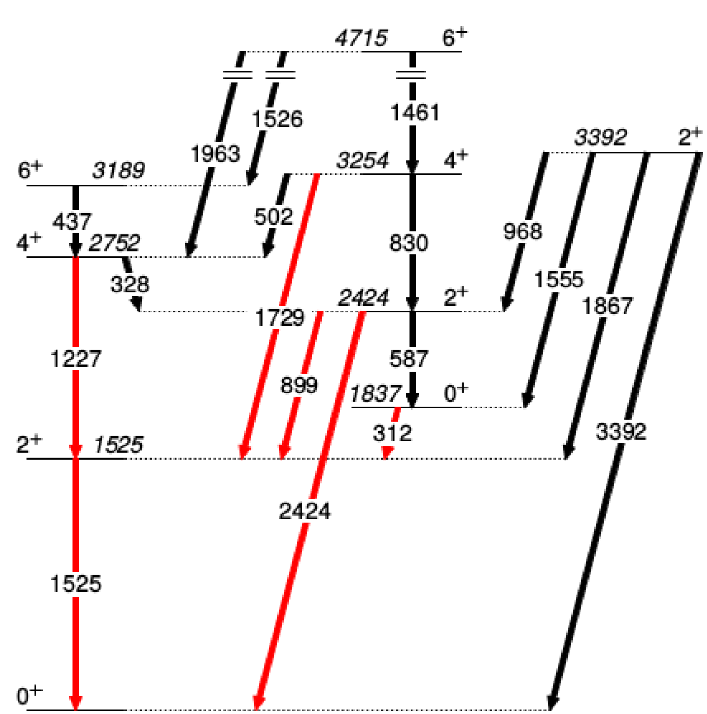

K. Hadyńska-Klęk, P. Napiorkowski, M. Zielińska *et al.*, PRL 117, 062501 (2016)

2 experiments, 9 gamma yields

10 branching ratios

9 lifetimes

2 mixing ratio

1 known quadrupole moment

26 ME
E2 and M1

Nuclear shapes in ^{42}Ca

TABLE II. Experimental and theoretical shape parameters $\langle Q^2 \rangle$ [e^{2}fm^4], $\sigma(Q^2)$ [e^{2}fm^4] and cos(3δ).

	Present
state	$\langle Q^2 \rangle$
$\mathbf{0}_1^+$	500 (20)
$\mathbf{2}_1^+$	900 (100)
$\mathbf{0}_2^+$	1300 (230)
$\mathbf{2}_2^+$	1400 (250)
	cos(3δ)
	Present
$\mathbf{0}_1^+$	$0.06^{+0.10}_{-0.10}$
$\mathbf{0}_2^+$	$0.79^{+0.13}_{-0.13}$

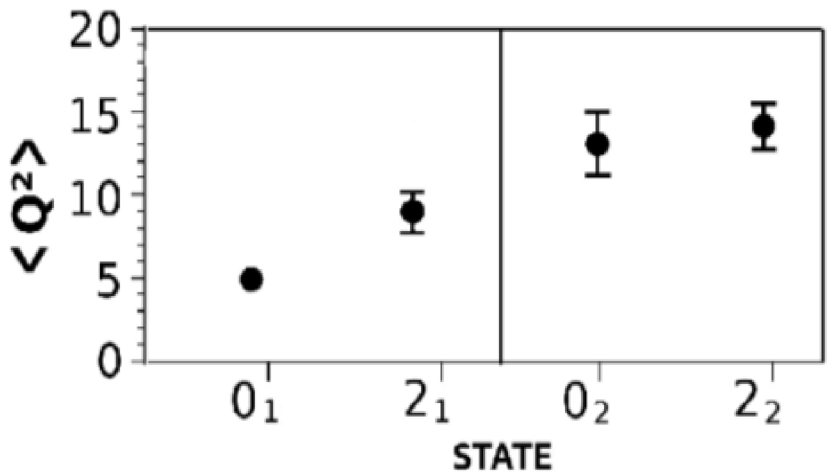

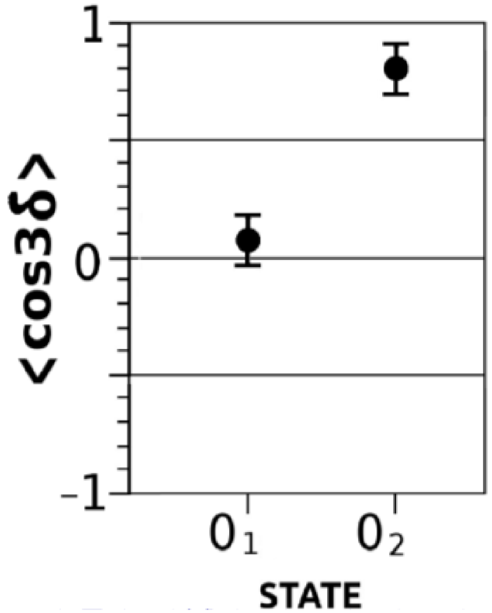

Nuclear shapes in ^{42}Ca

TABLE II. Experimental and theoretical shape parameters $\langle Q^2 \rangle$ [e^2fm^4], $\sigma(Q^2)$ [e^2fm^4] and $\cos(3\delta)$.

	Present
state	$\langle Q^2 \rangle$
$\mathbf{0_1^+}$	500 (20)
$\mathbf{2_1^+}$	900 (100)
$\mathbf{0_2^+}$	1300 (230)
$\mathbf{2_2^+}$	1400 (250)

cos(3δ)

	Present
$\mathbf{0_1^+}$	$0.06^{+0.10}_{-0.10}$
$\mathbf{0_2^+}$	$0.79^{+0.13}_{-0.13}$

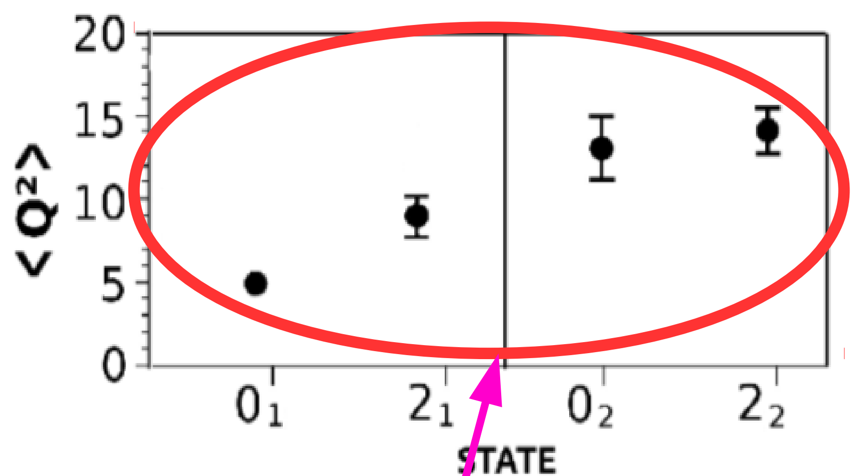

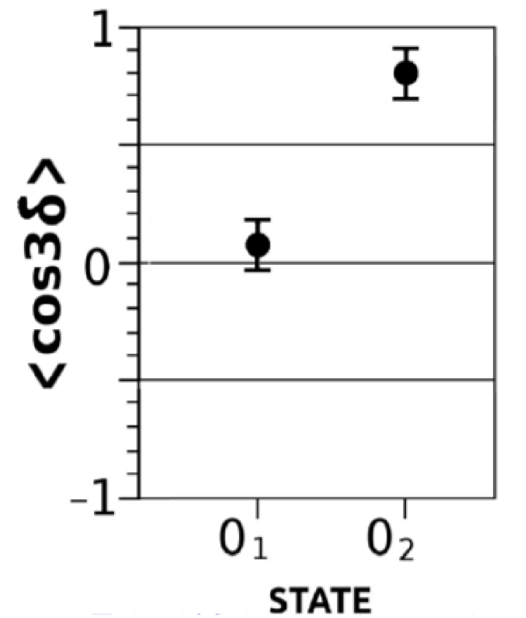

Increasing deformation in GSB and stable in the side band

Nuclear shapes in ^{42}Ca

cos(3δ)~0.8 – slightly triaxial 0_2

TABLE II. Experimental and theoretical shape parameters $\langle Q^2 \rangle$ [e^2fm^4], $\sigma(Q^2)$ [e^2fm^4] and $\cos(3\delta)$.

state	Present $\langle Q^2 \rangle$
0_1^+	500 (20)
2_1^+	900 (100)
0_2^+	1300 (230)
2_2^+	1400 (250)

	cos(3δ) Present
0_1^+	$0.06^{+0.10}_{-0.10}$
0_2^+	$0.79^{+0.13}_{-0.13}$

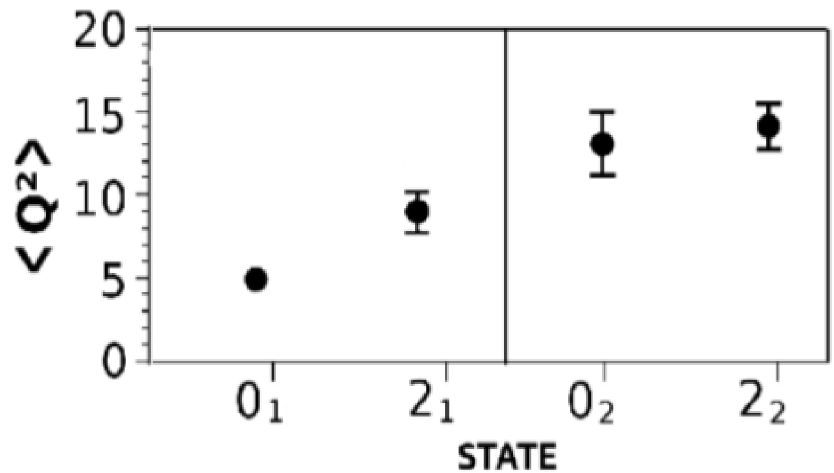

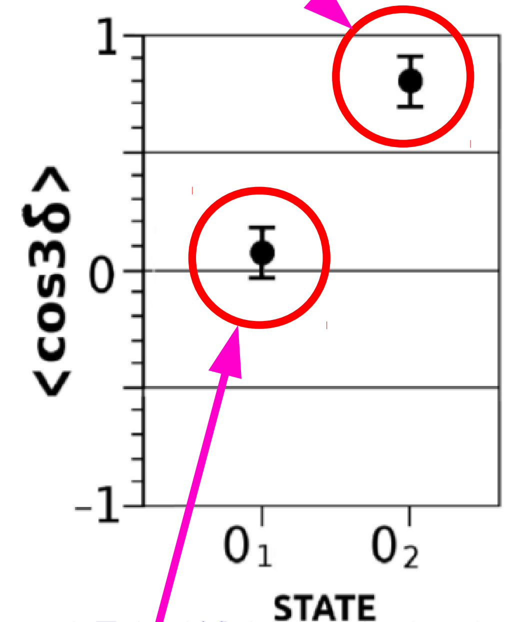

cos(3δ)~0 – triaxial GS??
In spherical ^{40}Ca region?

Nuclear shapes in ^{42}Ca

cos(3δ)~0.8 – slightly triaxial 0_2

TABLE II. Experimental and theoretical shape parameters $\langle Q^2 \rangle$ [e^2fm^4], $\sigma(Q^2)$ [e^2fm^4] and $\cos(3\delta)$.

state	Present $\langle Q^2 \rangle$
0_1^+	500 (20)
2_1^+	900 (100)
0_2^+	1300 (230)
2_2^+	1400 (250)

	cos(3δ) Present
0_1^+	$0.06^{+0.10}_{-0.10}$
0_2^+	$0.79^{+0.13}_{-0.13}$

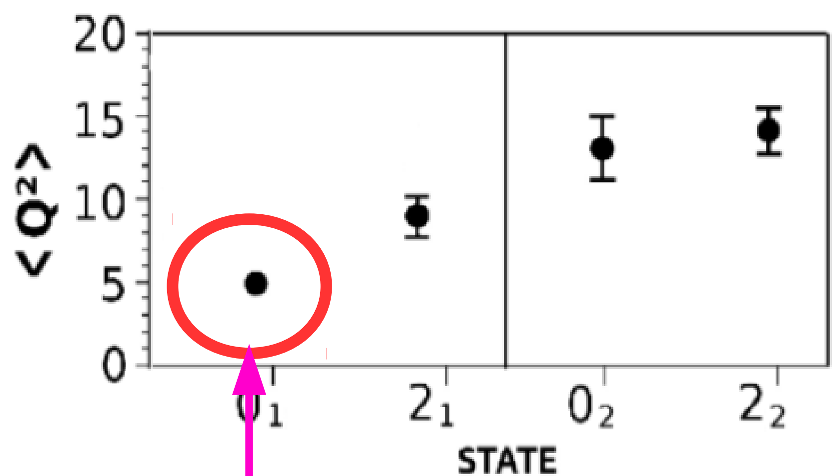

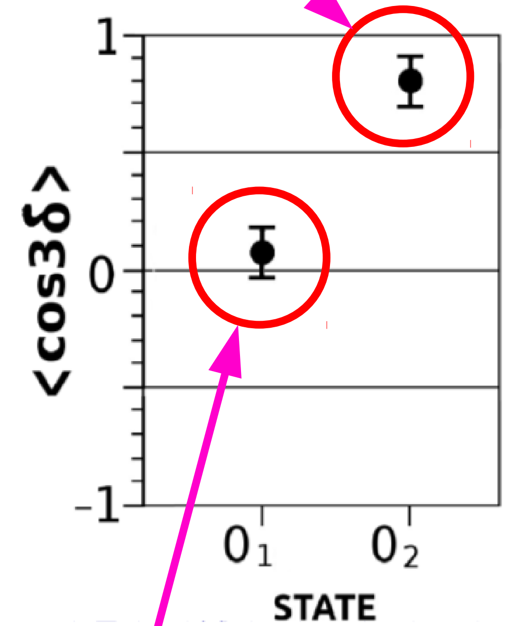

Non-zero deformation of the ground state?

cos(3δ)~0 – triaxial GS??
In spherical ^{40}Ca region?

SHAPE PARAMETERS

$$\frac{1}{\sqrt{5}}\langle Q^2\rangle = \frac{1}{\sqrt{2I_i+1}}\sum_t \langle i\|E2\|t\rangle\langle t\|E2\|f\rangle \begin{Bmatrix} 2 & 2 & 0 \\ I_i & I_f & I_t \end{Bmatrix}$$

$$\langle Q^3\cos(3\delta)\rangle = \mp\frac{\sqrt{35}}{\sqrt{2}}\frac{1}{\sqrt{2I_i+1}}\sum_{tu} \langle s\|E2\|u\rangle\langle u\|E2\|t\rangle\langle t\|E2\|s\rangle \begin{Bmatrix} 2 & 2 & 2 \\ I_s & I_t & I_u \end{Bmatrix}$$

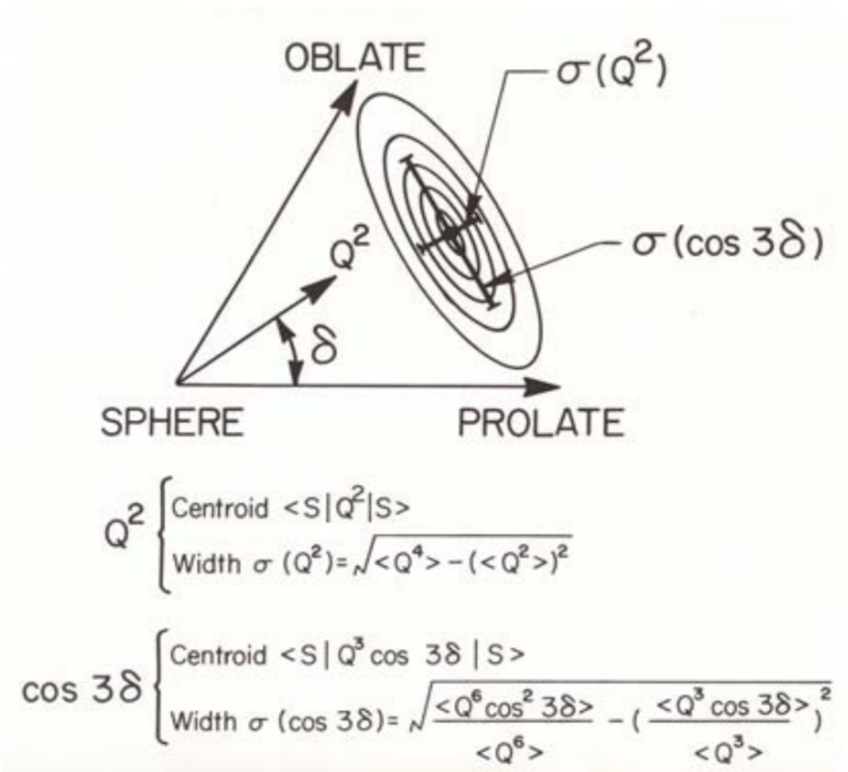

$$\beta = \sqrt{\langle\beta^2\rangle} = \sqrt{\frac{\langle Q^2\rangle}{q_0^2}},$$

$$\gamma = \arccos\langle\cos(3\delta)\rangle,$$

J. Srebrny and D. Cline, Int. J. Mod. Phys. E20, 422 (2011)

Nuclear shapes in ^{42}Ca

cos(3δ)~0.8 – slightly triaxial 0_2

TABLE II. Experimental and theoretical shape parameters $\langle Q^2 \rangle$ [e^2fm^4], $\sigma(Q^2)$ [e^2fm^4] and $\cos(3\delta)$.

	Present
state	$\langle Q^2 \rangle$
0_1^+	500 (20)
2_1^+	900 (100)
0_2^+	1300 (230)
2_2^+	1400 (250)

	cos(3δ)
	Present
0_1^+	$0.06^{+0.10}_{-0.10}$
0_2^+	$0.79^{+0.13}_{-0.13}$

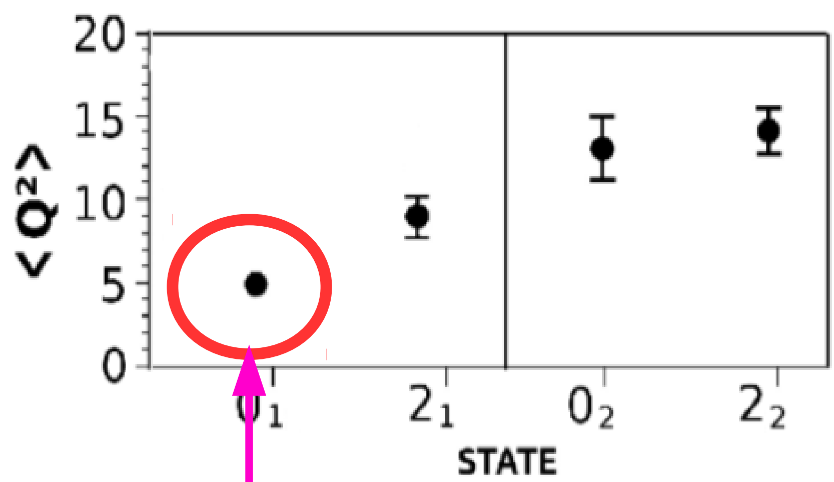

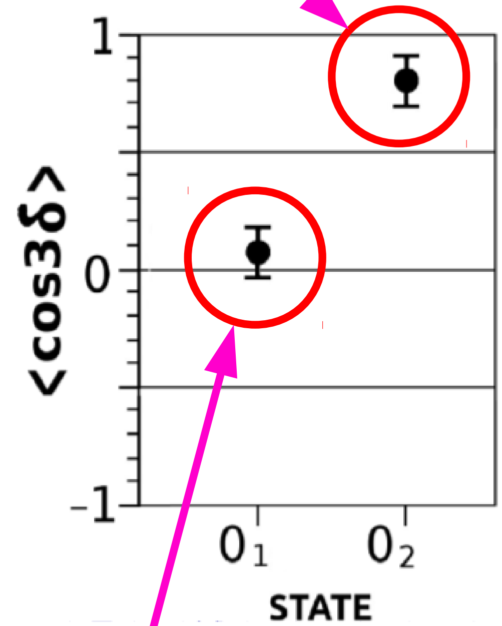

Non-zero deformation of the ground state?

cos(3δ)~0 – triaxial GS??
In spherical ^{40}Ca region?

0_1 β=0.26(2) and γ=29(2)°

0_2 β=0.43(2) and γ=13(6)°

Nuclear shapes in ^{42}Ca

cos(3δ)~0.8 – slightly triaxial 0_2

TABLE II. Experimental and theoretical shape parameters $\langle Q^2 \rangle$ [e^2fm^4], $\sigma(Q^2)$ [e^2fm^4] and $\cos(3\delta)$.

state	Present $\langle Q^2 \rangle$
0_1^+	500 (20)
2_1^+	900 (100)
0_2^+	1300 (230)
2_2^+	1400 (250)

state	cos(3δ) Present
0_1^+	$0.06^{+0.10}_{-0.10}$
0_2^+	$0.79^{+0.13}_{-0.13}$

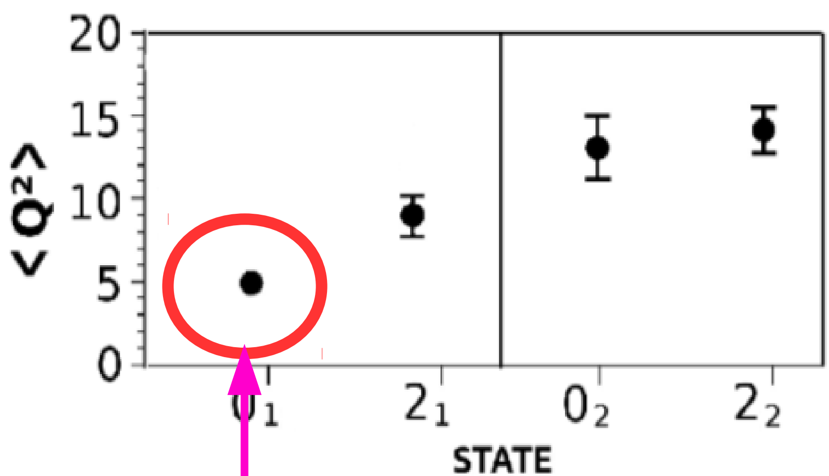

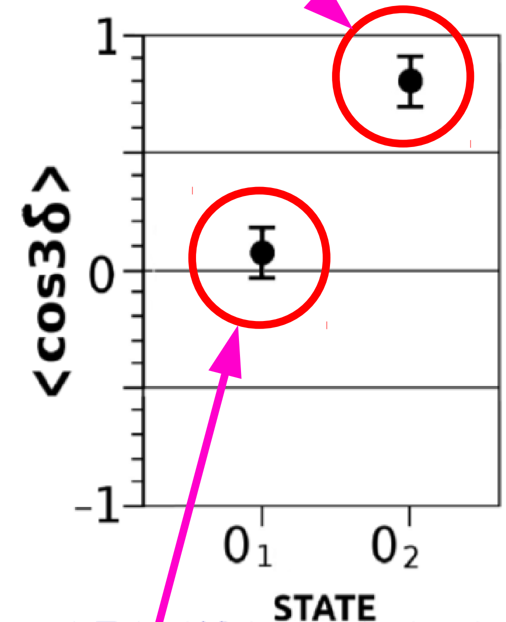

Non-zero deformation of the ground state?

0_1 β=0.26(2) and γ=29(2)°

0_2 β=0.43(2) and γ=13(6)°

cos(3δ)~0 – triaxial GS??
In spherical ^{40}Ca region?

What can we do?

Nuclear shapes in ^{42}Ca

Non-zero Q^2 for the ground state could be caused by **fluctuations** around the spherical shape...

If so, the maximum triaxiality could be the effect of averaging over **all possible shapes**.

How can we check it?

Nuclear shapes in ^{42}Ca

Non-zero Q^2 for the ground state could be caused by **fluctuations** around the spherical shape...

If so, the maximum triaxiality could be the effect of averaging over **all possible shapes**.

How can we check it?

The dispersion of Q^2 , $\sigma(Q^2)$, should be comparable to Q^2 value

Nuclear shapes in ^{42}Ca

Non-zero Q^2 for the ground state could be caused by **fluctuations** around the spherical shape...

If so, the maximum triaxiality could be the effect of averaging over **all possible shapes**.

How can we check it?

The dispersion of Q^2 , $\sigma(Q^2)$, should be comparable to Q^2 value

What is dispersion?

Nuclear shapes AGAIN

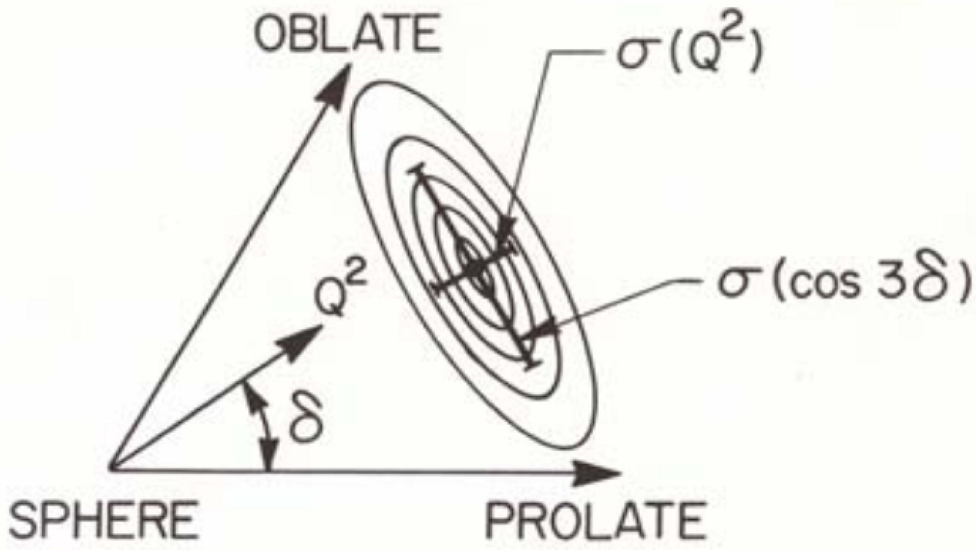

Q^2 Centroid: $\langle S|Q^2|S\rangle$

Q^2 Width: $\sigma(Q^2) = \sqrt{\langle Q^4\rangle - (\langle Q^2\rangle)^2}$

$\cos 3\delta$ Centroid: $\langle S|Q^3 \cos 3\delta|S\rangle$

$\cos 3\delta$ Width: $\sigma(\cos 3\delta) = \sqrt{\dfrac{\langle Q^6 \cos^2 3\delta\rangle}{\langle Q^6\rangle} - \left(\dfrac{\langle Q^3 \cos 3\delta\rangle}{\langle Q^3\rangle}\right)^2}$

$$\sigma(Q^2) = \sqrt{\langle Q^4\rangle - \langle Q^2\rangle^2}$$

Nuclear shapes in ^{42}Ca

The experimental data are insufficient... But we can try to use the theoretical predictions and the full set of ME from the calculations:

- Large Scale Shell Model (F. Nowacki, H. Naidja - Strasbourg)

- Beyond Mean Field (T. Rodriguez - Madrid)

Nuclear shapes in ^{42}Ca

The experimental data are insufficient... But we can try to use the theoretical predictions and the full set of ME from the calculations:

- **Large Scale Shell Model (F. Nowacki, H. Naidja - Strasbourg)**
- **Beyond Mean Field (T. Rodriguez - Madrid)**

LSSM

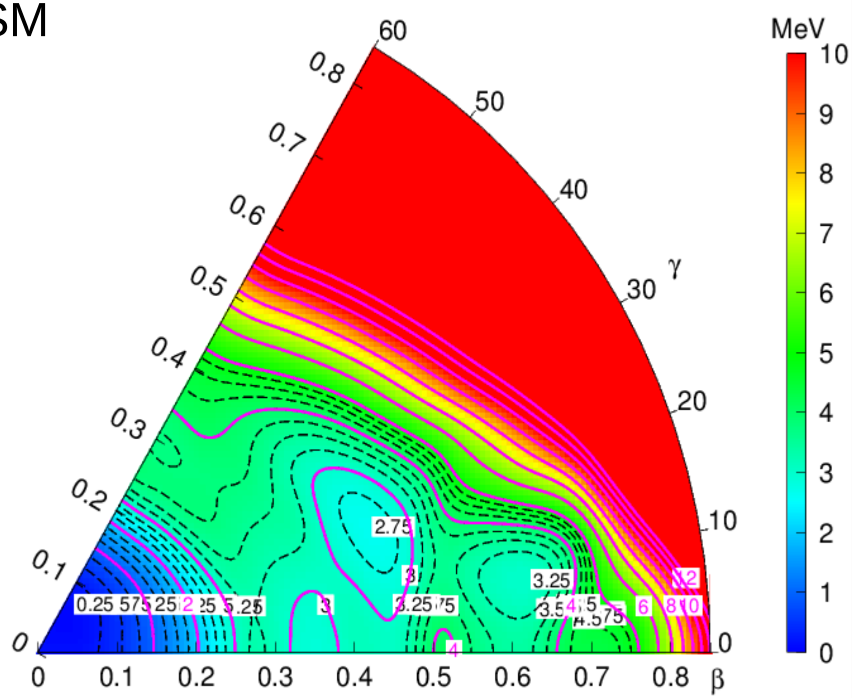

BMF

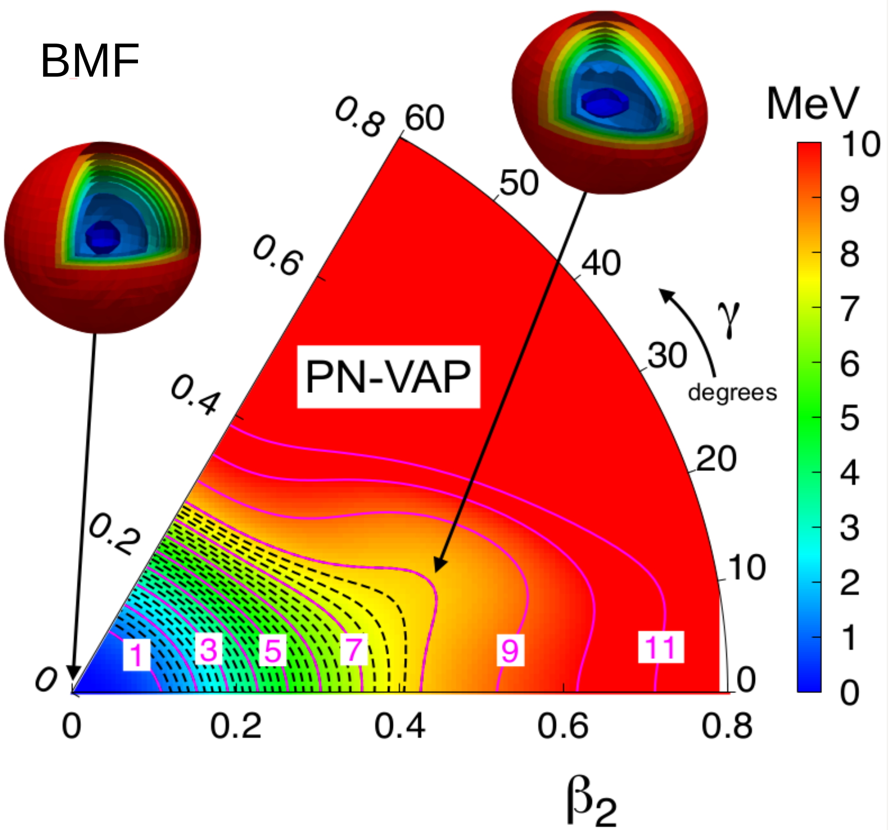

Nuclear shapes in ^{42}Ca

The experimental data are insufficient... But we can try to use the theoretical predictions and the full set of ME from the calculations:

- Large Scale Shell Model (F. Nowacki, H. Naidja - Strasbourg)

- Beyond Mean Field (T. Rodriguez - Madrid)

TABLE II. Experimental and theoretical shape parameters $\langle Q^2\rangle$ [e^2fm^4], $\sigma(Q^2)$ [e^2fm^4] and $\cos(3\delta)$.

	Present	LSSM		BMF	
state	$\langle Q^2\rangle$	$\langle Q^2\rangle$	$\sigma(Q^2)$	$\langle Q^2\rangle$	$\sigma(Q^2)$
0_1^+	500 (20[illegible]	300	500	100	300
2_1^+	900 (10[illegible])	300	500	100	300
0_2^+	1300 (23[illegible])	1460	400	1900	400
2_2^+	1400 (25[illegible])	1390	200	1900	300

	$\cos(3\delta)$		
	Present	LSSM	BMF
0_1^+	$0.06^{+0.10}_{-0.10}$	0.35	0.34
0_2^+	$0.79^{+0.13}_{-0.13}$	0.53	0.49

0_1 of ^{42}Ca is SPHERICAL with large fluctuations around minimum

0_2 state is SLIGHTLY TRIAXIAL/PROLATE shape

SIGMA

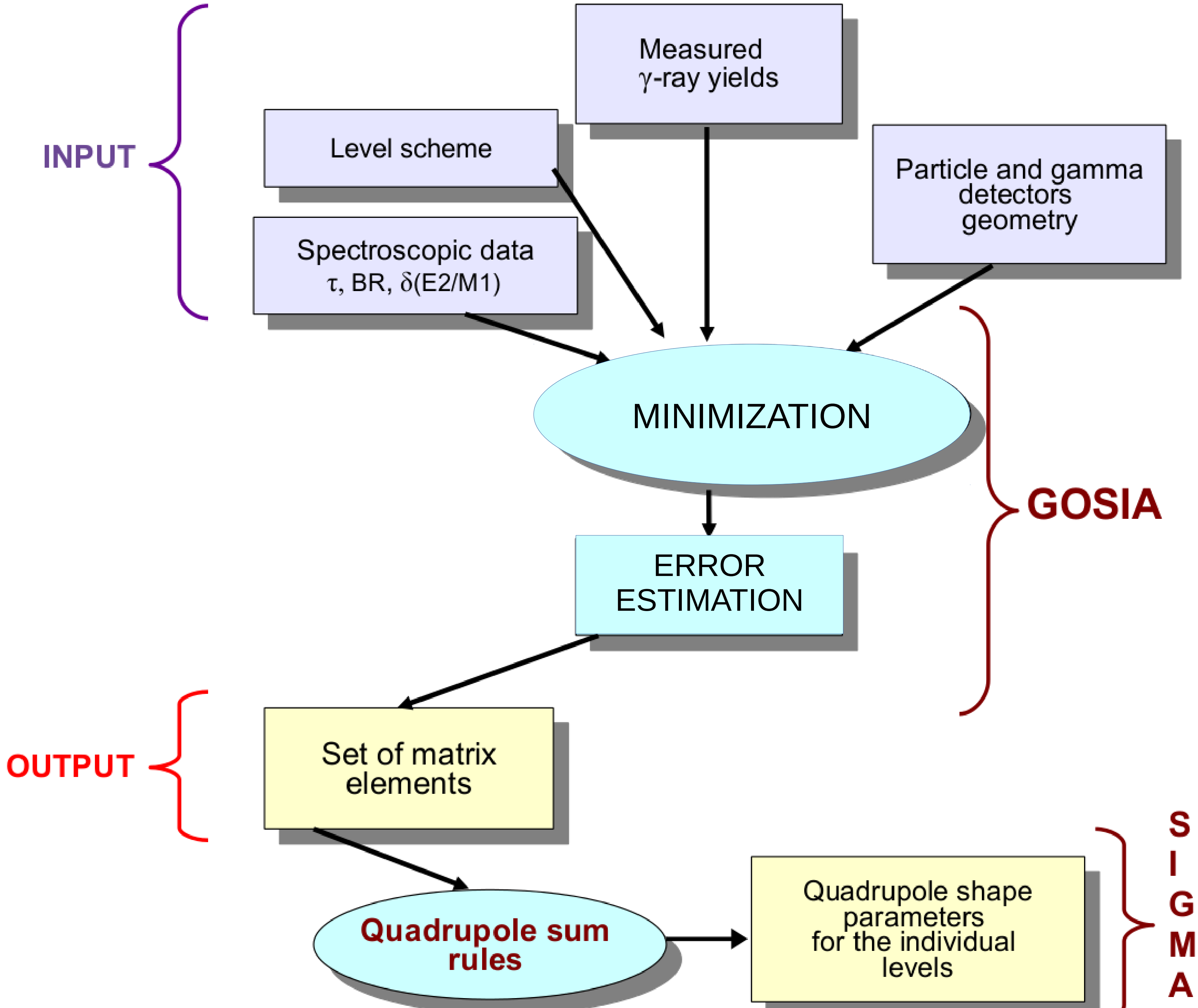

INPUT
Measured
γ-ray yields
Level scheme
Particle and gamma
detectors
geometry
Spectroscopic data
τ, BR, δ(E2/M1)
MINIMIZATION
GOSIA
ERROR
ESTIMATION
OUTPUT
Set of matrix
elements
Quadrupole sum
rules
Quadrupole shape
parameters
for the individual
levels
S
I
G
M
A

SIGMA

- Is a separate **fortran** program (you need to compile it like GOSIA)
- Very useful tool to **evaluate the Quadrupole Sum Rule Method**
- SIGMA uses the **output files from GOSIA** but can be also used separately (for expectation values estimation)
- Calculates the **shape invariants** and estimates their errors (if asked)
- Input is not complicated
- Output is full of information

SIGMA

- You must run OP,ERRO in GOSIA to get **TAPE3** (if CONT SMR, TAPE3 contains the output file for sum rules, IDF=1) and **TAPE15**
- You must run OP,SIXJ in GOSIA to calculate the table of 6j coefficients (output file **TAPE14**) (can be inserted anywhere in the input file, even as the only option)

SIGMA

- You must run OP,ERRO in GOSIA to get **TAPE3** (if CONT SMR, TAPE3 contains the output file for sum rules, IDF=1) and **TAPE15**
- You must run OP,SIXJ in GOSIA to calculate the table of 6j coefficients (output file **TAPE14**) (can be inserted anywhere in the input file, even as the only option)

sigma.inp

```
IL
NST
TAPE3.smr
TAPE15.err
TAPE14.tab
```

SIGMA

- You must run OP,ERRO in GOSIA to get **TAPE3** (if CONT SMR, TAPE3 contains the output file for sum rules, IDF=1) and **TAPE15**
- You must run OP,SIXJ in GOSIA to calculate the table of 6j coefficients (output file **TAPE14**) (can be inserted anywhere in the input file, even as the only option)

sigma.inp

```
IL
NST
TAPE3.smr
TAPE15.err
TAPE14.tab
```

IL: 1 – printout of the ME involved in evaluation of all shape invariants
0 – for the simpler output

SIGMA

- You must run OP,ERRO in GOSIA to get **TAPE3** (if CONT SMR, TAPE3 contains the output file for sum rules, IDF=1) and **TAPE15**
- You must run OP,SIXJ in GOSIA to calculate the table of 6j coefficients (output file **TAPE14**) (can be inserted anywhere in the input file, even as the only option)

sigma.inp

```
IL
NST
TAPE3.smr
TAPE15.err
TAPE14.tab
```

The mode of error calculations
-1 – no error estimation (SIGMA can be independent from GOSIA if you use this option)
0 – errors will be calculated only for Q2, three values of v(Q2) and four of cos3d for each state
99 – error will be calculated for each statistical moment (too long and complicated)

SIGMA

- You must run OP,ERRO in GOSIA to get **TAPE3** (if CONT SMR, TAPE3 contains the output file for sum rules, IDF=1) and **TAPE15**
- You must run OP,SIXJ in GOSIA to calculate the table of 6j coefficients (output file **TAPE14**) (can be inserted anywhere in the input file, even as the only option)

sigma.inp

```
IL
NST
TAPE3.smr
TAPE15.err
TAPE14.tab
```

```
0
0
TAPE3.smr
TAPE15.err
TAPE14.tab
```

IL: 1 – printout of the ME involved in evaluation of all shape invariants
0 – for the simpler output

NST: The mode of error calculations
-1 – no error estimation (SIGMA can be independent from GOSIA if you use this option)
0 – errors will be calculated only for Q2, three values of v(Q2) and four of cos3d for each state
99 – error will be calculated for each statistical moment (too long and complicated)

SIGMA.OUT

```
**************************************************************************************
  INDEX= 5    SPIN= 0.0    ENERGY= 1.8370

**************************************************************************************
     Q2           ERROR
  0.1313     -0.0233     0.0281
----------------------------------------------------------------------
     Q4(0)   VARIANCE          ERROR        SQRT(VAR)       ERROR        SQRT(VAR)/Q2       ERROR
  0.0185      0.0012     -0.0002     0.0002     0.0349     -0.0033     0.0033     0.2656     -0.0254     0.0251
----------------------------------------------------------------------
     Q4(2)   VARIANCE          ERROR        SQRT(VAR)       ERROR        SQRT(VAR)/Q2       ERROR
  0.0292      0.0120     -0.0062     0.0061     0.1095     -0.0333     0.0249     0.8337     -0.2539     0.1895
----------------------------------------------------------------------
     Q4(4)   VARIANCE          ERROR        SQRT(VAR)       ERROR        SQRT(VAR)/Q2       ERROR
  0.0174      0.0002     -0.0053     0.0035     0.0124   **********   0.0481     0.0945   **********   0.3662
     Q6(0)   SKEWNESS          ERROR
  0.0026     -0.0001      0.0000     0.0000
----------------------------------------------------------------------
     Q6(2)   SKEWNESS          ERROR
  0.0053     -0.0017      0.0000     0.0000
----------------------------------------------------------------------
     Q6(4)   SKEWNESS          ERROR
  0.0027      0.0003      0.0000     0.0000
----------------------------------------------------------------------
     Q3COS(3D)   COS(3D)        ERROR         INT.Q3
  0.0385      0.7882     -0.1262     0.1257     0.0488
----------------------------------------------------------------------
     Q5COS(3D)(0) COS(3D)        ERROR          INT.Q5
  0.0051      0.7275     -0.1311     0.1240     0.0070
----------------------------------------------------------------------
     Q5COS(3D)(2) COS(3D)        ERROR          INT.Q5
  0.0034      0.2763     -0.1246     0.1608     0.0123
----------------------------------------------------------------------
     Q5COS(3D)(4) COS(3D)        ERROR          INT.Q5
  0.0044      0.6573     -1.7129     0.8310     0.0067
----------------------------------------------------------------------
     <COS2(3D)>(1) VARIANCE      ERROR        SQRT(VAR)        ERROR
  0.5604     -0.0609      0.0000     0.0000     0.0000     0.0000     0.0000
----------------------------------------------------------------------
     <COS2(3D)>(2) VARIANCE      ERROR        SQRT(VAR)        ERROR
  0.4387     -0.1825      0.0000     0.0000     0.0000     0.0000     0.0000
----------------------------------------------------------------------
     <COS2(3D)>(3) VARIANCE      ERROR        SQRT(VAR)        ERROR
  0.7389      0.1176      0.0000     0.0000     0.3430     0.0000     0.0000
```

$$\sigma(Q^2) = \sqrt{\langle Q^4\rangle - \langle Q^2\rangle^2}$$

The dispersion of Q^2

Conclusions

- Quadrupole sum rules method allows to study **nuclear shapes** in **different states**
- It can be useful when you want to **compare** the **experimental results with theory**
- **SIGMA works with GOSIA** → fast calculations of nuclear shapes

(→ *hands-on session*)

Conversion electrons in GOSIA

- Coulex cross section calculation → matrix elements determined from the γ-ray decay.
- A competetive to γ-ray emission is another electromagnetic process → internal conversion.
- Usually electrons are not measured in Coulex run → GOSIA evaluates the loss in conversion.
- OP, YIEL in GOSIA → **Internal Conversion Coeffcients** for the **Eλ** and **Mλ** transitions.

$\alpha = \lambda_e / \lambda_\gamma$ the ratio of the decay probability arising from γ emision (λ_γ) and from electron emision (λ_e).

- A nonrelativistic calculation gives the analytic relations for α:

$$\alpha(EL) \cong \frac{Z^3}{n^3}\left(\frac{L}{L+1}\right)\left(\frac{e^2}{4\pi\epsilon_0\hbar c}\right)^4\left(\frac{2m_ec^2}{E}\right)^{L+5/2}$$

$$\alpha(ML) \cong \frac{Z^3}{n^3}\left(\frac{e^2}{4\pi\epsilon_0\hbar c}\right)^4\left(\frac{2m_ec^2}{E}\right)^{L+3/2}$$

Depend on :
- element (Z)
- the multipolarity
- γ-ray energy

The probability decreases rappidly with energy → *Z* = 80, *E2* transitions **α = 136** @ 50 keV
= **5.5** @ 100 keV
= **2.7 10^{-2}** @ 500 keV

Courtesy of K. Wrzosek-Lipska, HIL Warsaw

A special case: the *E0* transition (1/2)

- Occur between states of the same spin and parity and no momentum is transferred.
- Cannot occur in the emission of a single photon.
- Energy is transferred to a high energy atomic electron.

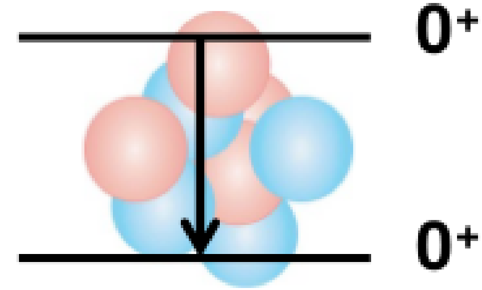

Transition probability:

$$W(\mathrm{E0}) = \frac{1}{\tau(\mathrm{E0})} = \rho^2(\mathrm{E0}) \times [\Omega_{\mathrm{ic}}(\mathrm{E0}) + \Omega_{\pi}(\mathrm{E0})]$$

monopol transition strength

„electronic" (non-nuclear) factors

Monopole transition strength:

$$\rho(\mathrm{E0}) = \frac{\langle f|M(\mathrm{E0})|i\rangle}{eR^2}$$

monopole matrix element

nuclear radius

The probability to decay through the *E*0 transition contains ***nuclear structure information*** that GOSIA cannot estimate.

T. Kibedi, R.H. Spear Atomic Data and Nuclear Data Tables 89 (2005) 77–100
J. L. Wood et al., Nuclear Physics A 651 (1999) 323-368

Courtesy of K. Wrzosek-Lipska, HIL Warsaw

E0 transition in the GOSIA analysis

N. Bree PhD thesis, KU Leuven 2014

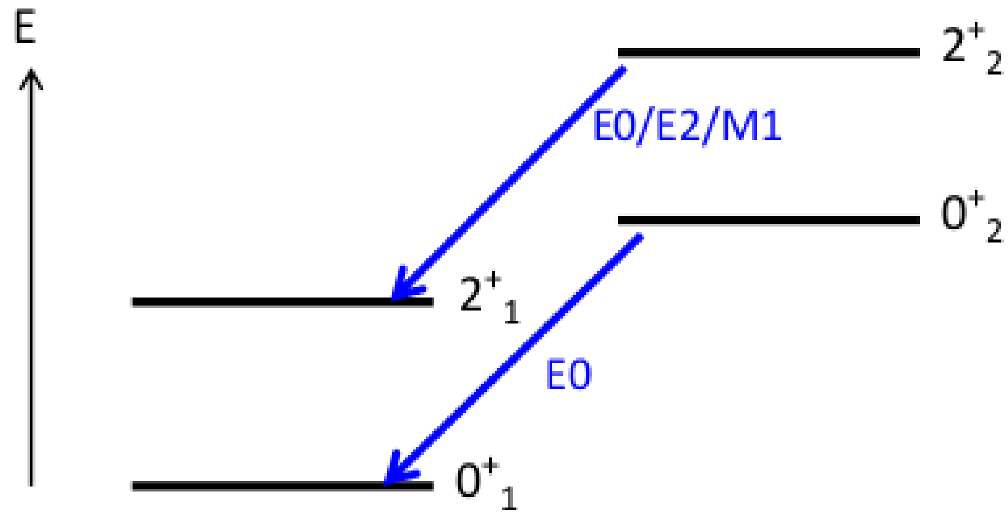

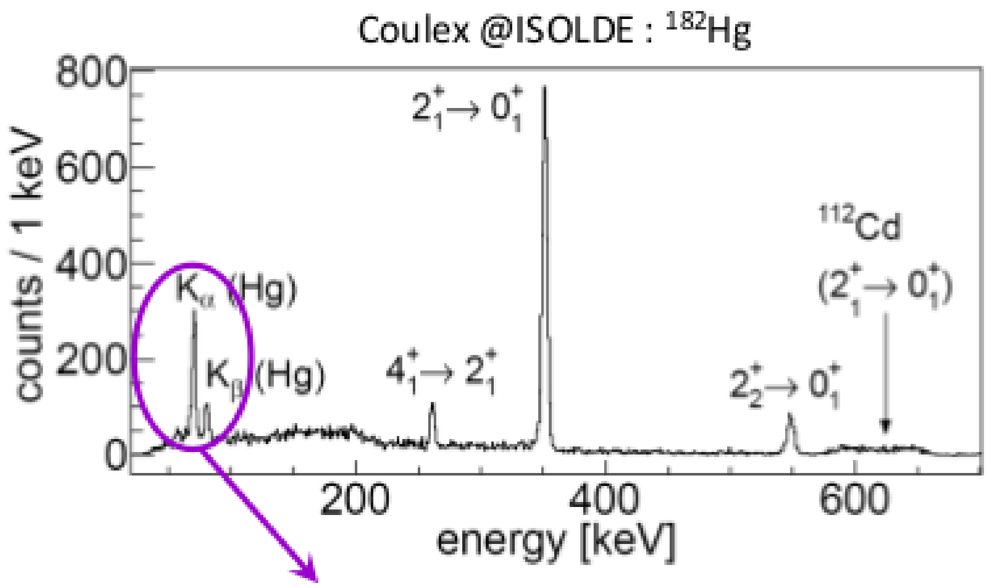

- conversion of E2/M1 γ's
- atomic production of K vacancy in ion-atom collision
  N. Bree et al., NIM B360 (2015) 97
- the *E0* transitions $0^+_2 \rightarrow 0^+_1$, $2^+_2 \rightarrow 2^+_1$

- The decay of the 0^+_2, 2^+_2 can occur through a gamma (E2, M1) or an electron (E0).
- Electrons are not measured in Coulex and the ***E0* is not included** in the de-excitation.
- In heavy nuclei (e.g. **Pb region**) low-energy transitions can be **strongly converted**.
- For GOSIA, the 2^+_2 will decay only through the E2 or M1 transition.

Courtesy of K. Wrzosek-Lipska, HIL Warsaw

E0 transition in the GOSIA analysis

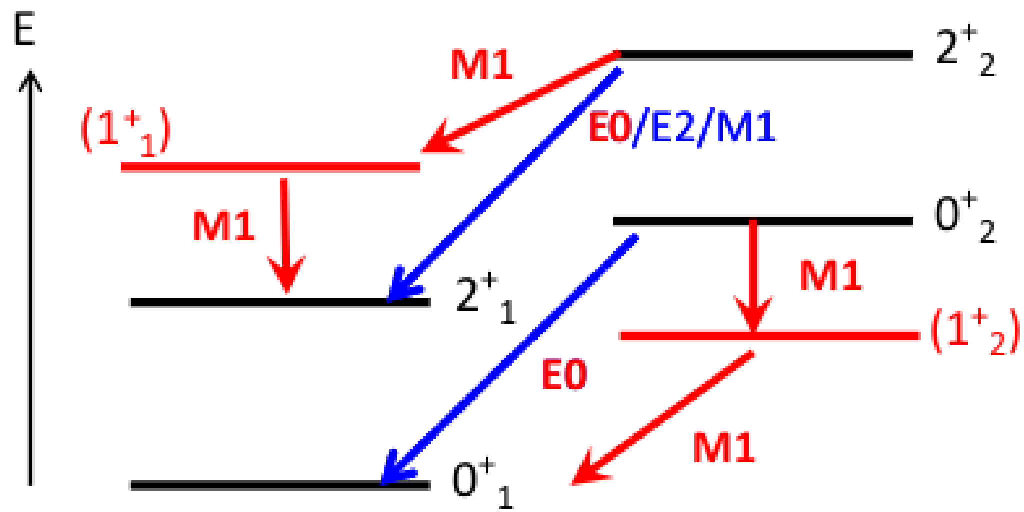

- declare a ≪ virtual ≫ state (e.g. 1^+) in the LEVE section;
- declare the *M*1 matrix elements connecting 1^+ states with the 2^+ and 0^+ states (NOTE → the 1^+ state will not be populated in the excitation);
- "fake" *M*1 transitions **simulate *E*0 -decay** of the 2^+_2 and 0^+_2 states to the 2^+_1 and 0^+_1, respectively;
- declare the *E*0 yields in the yield file as a $0^+_2 \rightarrow 1^+_2$ and $2^+_2 \rightarrow 1^+_1$ transitions.

Courtesy of K. Wrzosek-Lipska, HIL Warsaw

Spectroscopic data related with the *E0* decay

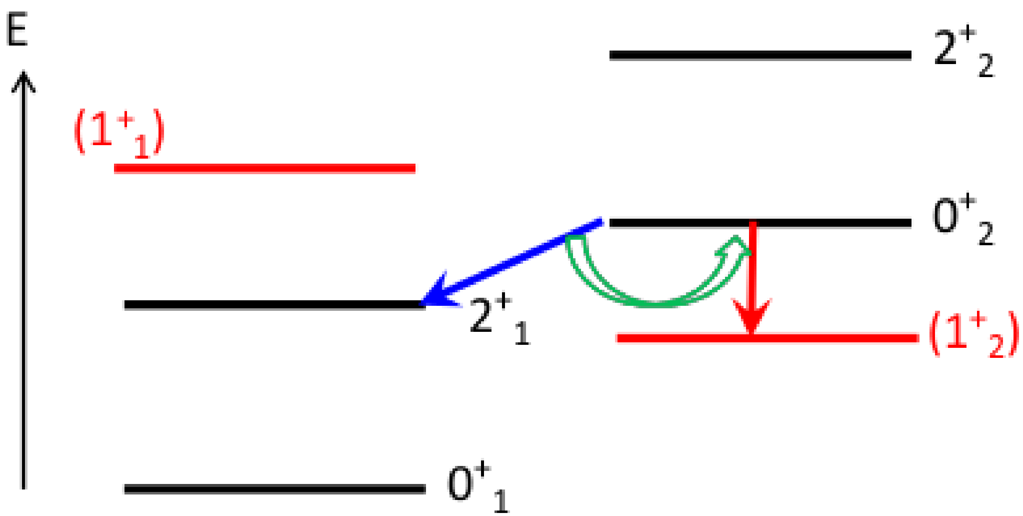

Available spectroscopic data related with the *E0* decay,

e.g. **BR (E2; $0^+_2 \rightarrow 2^+_1$) / (E0; $0^+_2 \rightarrow 2^+_1$)** can be declared

in Gosia as additional data point.

These are expressed through the relevant matrix elements.

Recent case for GOSIA: Mo, Kr, Hg, Po, Pb

Courtesy of K. Wrzosek-Lipska, HIL Warsaw

Nuclei characterized by **coexisting shapes** having different deformations will exhibit **strong $\rho^2\ (E0)$** values if the states associated with the coexisting shapes become **mixed.**

J. L. Wood et al., Nuclear Physics A 651 (1999) 323-368

Courtesy of K. Wrzosek-Lipska, HIL Warsaw

Two-state mixing model

"Nuclear Structure from a Simple Perspective", R.F. Casten, Oxford University Press

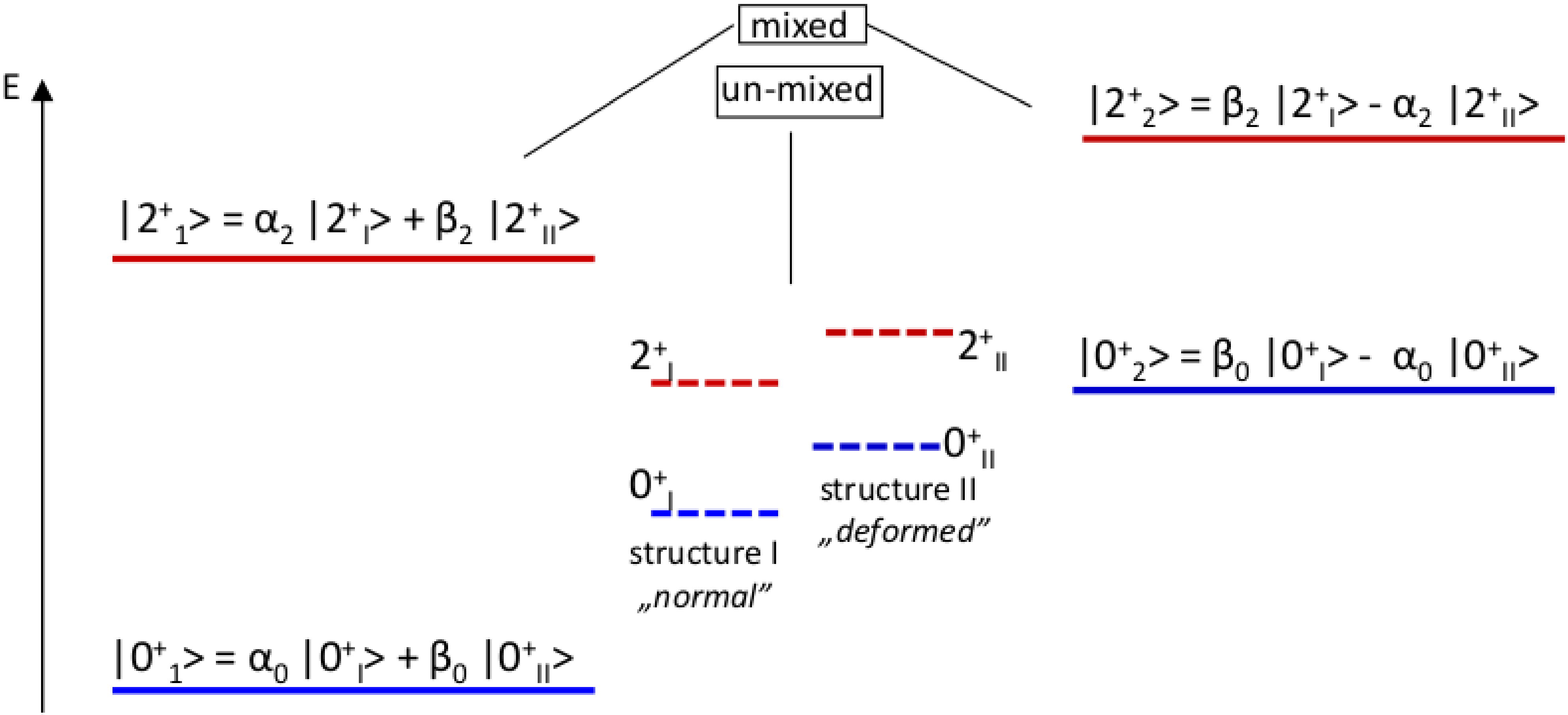

$$\alpha_J^2 + \beta_J^2 = 1$$

The relative position of the mixed states depends on the **unperturbed energy difference** and on the **strength of the mixing interaction V**

Courtesy of K. Wrzosek-Lipska, HIL Warsaw

Two-state mixing model

"Nuclear Structure from a Simple Perspective", R.F. Casten, Oxford University Press

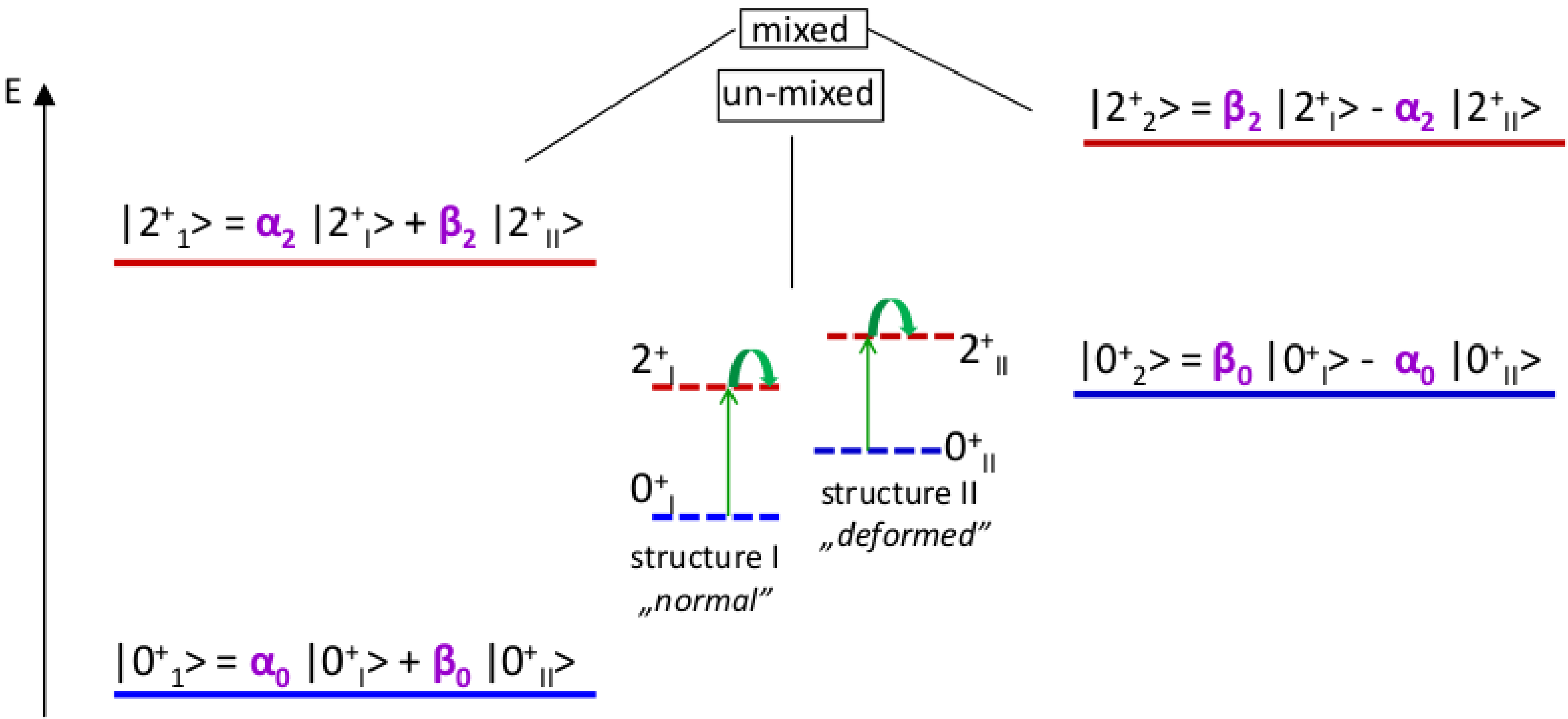

$$\langle J^\pi_I \| E2 \| J^\pi_{II} \rangle = 0$$

$$\alpha_J^2 + \beta_J^2 = 1$$

Experimental *E*2 matrix elements can be expressed by:

- un-mixed *E*2 matrix elements
- **mixing amplitudes ($\alpha_0, \alpha_2, \beta_0, \beta_2$)** → fit to the energy levels (VMI model)

Courtesy of K. Wrzosek-Lipska, HIL Warsaw